QED IN HIGHLY-CHARGED, HIGH Z IONS — EXPERIMENTS AT THE STORAGE RING ESR*

P.H. MOKLER

GSI - Darmstadt, Germany

(Received December 8, 1995)

A survey on the fundamental structure aspects of very heavy few-electron ions, in particular H-like systems, is presented. Special emphasis is given to contributions from quantum-electro-dynamics at strong central potentials. The technical possibilities to produce highly-charged heavy ions are reviewed and the ground-state Lamb-shift experiments performed at the heavy ion storage ring ESR are summarized. A short outlook on further developments in this field is added.

PACS numbers: 25.90.+k

Structure of heavy few-electron ions

The structure of atoms was first revealed within Bohr's atomic model around 1913. There, the binding energy of an electron, E_n, in a one-electron atom, *i.e.* a H-like ion, was given by the Rydberg formula:

$$E_n = \frac{\mathrm{Ry}\, Z^2}{n^2},$$

where Z is the atomic number, n the shell number, and Ry = 13.6 eV the Rydberg constant. Around 1930 the atomic structure seemed to be understood precisely within the wave description of the quantum mechanics developed by Schrödinger and Dirac for the non-relativistic and relativistic case, respectively. Only in 1947, Lamb and Retherford [1] discovered in the H atom a tiny splitting between the "degenerate" $2s_{1/2}$ and $2p_{1/2}$ levels. This Lambshift was finally explained within the framework of the

* Presented at the XXIV Mazurian Lakes School of Physics, Piaski, Poland, August 23–September 2, 1995.

quantum-electro-dynamics. These QED effects can be visualized by the so-called Feynman diagrams, showing the coupling of the bound electron to the fluctuations of the field. In Fig. 1 the atomic structure for hydrogenic atoms according to the different descriptions is given. Additionally, the radiative transitions for a real atom are indicated. The E1 transitions correspond to the Lyman-α lines; the magnetic transition, labeled M1, are only active in heavy ions due to the spin interaction — however, there these spin-flip transitions are very fast.

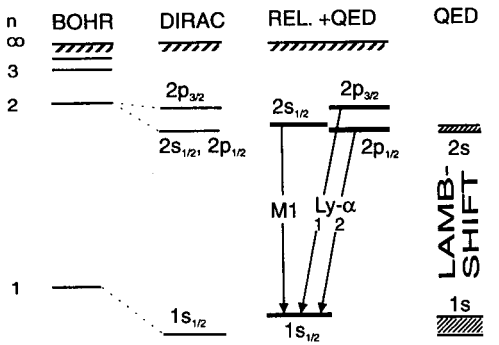

Fig. 1. The atomic structure of H-like atoms according to Bohr, Dirac, and including the QED contributions. For the latter realistic case, the radiative transitions from the L shell to the ground-state are indicated. At the right side the Lamb-shift contributions are given separately.

As was elucidated by the Rydberg formula, the binding energies for a certain shell increase quadratically with Z. In contrast the relativistic fine-structure splitting as well as the Lamb-shift increase with Z^4/n^3. This can also be read from Fig. 2, where the normalized transition energies from the L shell to the ground-state are given as a function of Z, both for H-like and He-like species. In this representation the structure is reduced by the overlaying Z^2 dependence. Due to the strong electron–electron interaction in light ions compared to the central field the structure for He-like ions deviates considerably from H-like species. However, for high atomic numbers Z the structure for He-like ions approaches a hydrogenic character as the central potential gets so dominant.

In the following we will mainly concentrate on H-like heavy ions. Hence, for an overview the typical energies involved in a H atom and in a H-like U ion are compared: the Lyman-α transition energies are about 10 eV and 100 keV, respectively; the fine-structure splitting in the L shell is about 45 μeV and 4.6 keV, the 2s Lamb-shift about 4.4 μeV and 75 eV, and the ground-state Lamb-shift 35 μeV and 463 eV, respectively. It is exactly this last quantity which gives for heavy ions access to the QED contributions in

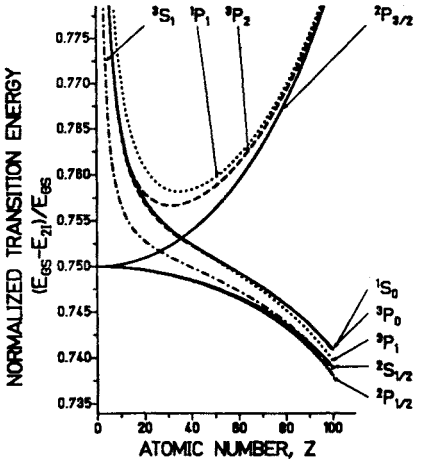

Fig. 2. Reduced transition energies from the L shell normalized to the ground-state binding energy for H-like (solid lines) and He-like (broken lines) ions as a function of the atomic number, acc. to Ref. [2].

strong atomic fields. For instance, the K electron in U feels a central field of typically 10^{15} V/cm and more.

According to Johnson and Soff [3] the Lamb-shift can be described accurately by a $Z\alpha$ expansion:

$$L_{ns} = \text{const.}\,\alpha\,\frac{(Z\alpha)^4}{n^3}\,F(Z\alpha)\,,$$

where $F(Z\alpha)$ is given as a power series expansion and α is the fine-structure constant. In Fig. 3 the result is reproduced including the main contributions to the ground-state Lamb-shift. We have two QED contributions, the self energy (SE) and the vacuum polarization (VP) and a more trivial part which takes care of the finite nuclear size corrections (NS). The Lamb-shift is usually defined as the deviation of the reality from the Dirac expectation value for a point-like nucleus. The self energy is the dominant part of the Lamb-shift; it can be characterized by the emission and reabsorption of a virtual photon by the bound electron, see the graph at top left in Fig. 3. The vacuum polarization, which corresponds to the coupling of the bound electron to a virtual positron-electron pair (see top right graph in Fig. 3) is only important for the heaviest ions, where also the nuclear size effect gets dominant. It has to be emphasized, that beyond about $Z = 40$ the higher order coefficients in the $F(Z\alpha)$ expansion start to dominate the QED contribution [4]. These terms cannot be measured for light ions, even with the enormous precision achieved with Doppler-free two-photon laser

spectroscopy for H atoms [5]. Hence, the Lamb-shift in strong fields, *i.e.* in very heavy ions, reveals higher order effects. The ground-state Lamb-shift is determined by a precision measurement of the ground-state transition energies (*cf.* Fig. 1) diminished by the Dirac expectation values.

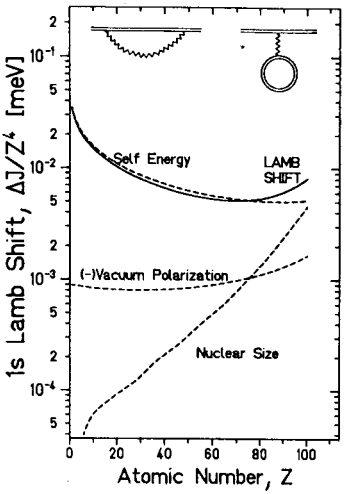

Fig. 3. Contributions to the ground-state Lamb-shift in H-like ions scaled by the general Z^4 dependence (acc. to Ref. [3]). The different QED contributions — self energy (top left graph) and vacuum polarization (top right graph), as well as the nuclear size effect — are given separately.

Production of very heavy few-electron ions

In order to be able to measure the ground-state transitions in H-like and He-like ions one has to produce these ultimately charged ions. This can be done efficiently only by electronic or atomic collisions. The electron impact ionization method is utilized in EBIT devices [6]. As the abbreviation tells — EBIT = Electron Beam Ion Trap — in those devices ions confined in a trap by electric and magnetic fields will successively be ionized to higher and higher charge states by intense, continuous and energetic electron impact. The principle of the layout of this almost table-top device is shown within the magnifying glass in Fig. 4. Unfortunately, due to recombination and other loss process, the number of ultimately charged very heavy ions is limited. In the Super-EBIT a few tens of bare U ions could be produced [7]. These ions are almost at rest, which is ideal for spectroscopic purposes as the Doppler effect will not limit the final accuracy. However, still the luminosity of this source is too weak for a detailed spectroscopic study of

e.g. H-like Uranium. Moreover, the charge-state mixture present in the trap also limits those investigations.

The other method, the stripping technique, uses atomic collisions for ionization. Low-charged ions are accelerated to high energies where they are stripped by penetrating a thin foil to high charge states according to their velocities. The higher the velocity is, the higher is the final charge state. In order to strip Uranium to bare species, one has to have energies beyond 300 MeV/u and the acceleration-stripping technique has to be applied in several stages as is indicated in Fig. 4. Finally, charge-state selected, ultimately-charged fast heavy ions will be injected into a storage ring where these ions are confined to closed orbits by magnetic guidance fields. In the storage ring these charge-state pure, however, fast ions can be accumulated to high intensities and provided for experiments. In the heavy ion synchrotron — storage ring facility, SIS-ESR, at GSI in Darmstadt up to 10^8 bare U ions have been used already for experiments.

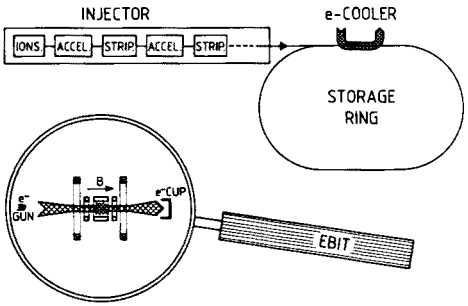

Fig. 4. Techniques to produce ultimately-charged, heavy ions: In the EBIT device (within the magnifying glass), trapped ions are successively ionized by continuous bombardment of energetic electrons. In the accelerator device, accelerated fast ions are stripped in foils to high charge states before they are trapped in a storage ring.

The experimental storage ring ESR is the only one that can store all bare ions up to naked Uranium. In Fig. 5 the layout of the GSI heavy ion facility is shown schematically in the overview at the top. The linear accelerator, the UNILAC with a length of about 120 m, accelerates the ions up to 11.4 MeV/u. After stripping the ions are boosted in the synchrotron, SIS with a circumference of 216 m, up to energies of 1000 MeV/u before final stripping. Bare ions up to 500 MeV/u Uranium are finally injected into the heavy ion storage ring, ESR, showing a hexagonal shape of the closed orbit with a perimeter of 108 m. More details of the ESR are shown in the bottom part of Fig. 5.

A crucial feature of all ion storage rings are their electron cooling devices (2). Due to the production of the fast ions injected (1) into a ring, the stored ion beams have a certain emittance, *i.e.* not all the ions have exactly

the same velocity vector. They show a narrow distribution around the average direction and the absolute value, which can be interpreted by a co-moving observer as a temperature. The absolute velocity distribution of the coasting ions can be measured as a distribution of the revolution frequencies by a so-called Schottky-noise pick-up probe. Such a frequency spectrum is displayed for coasting bare Uranium ions by the broad distribution in the central insert in Fig. 5 (the zero point is widely suppressed). These hot ions can now be effectively cooled by a beam of merged, co-moving cold electrons [8]. By elastic electron-ion collisions the ions temperature is quickly reduced by more than one or two orders of magnitude as is depicted by the narrow frequency distribution in the central insert (*cf.* Ref. [9]).

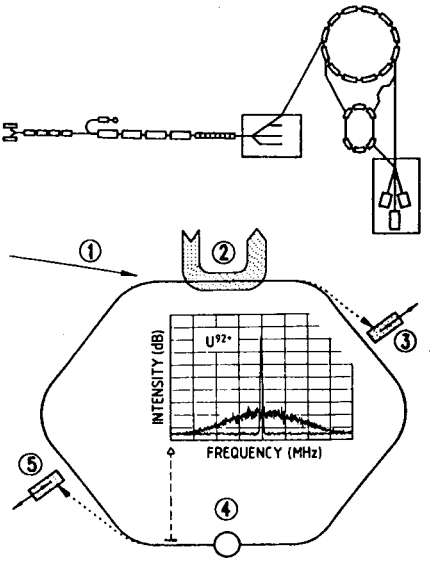

Fig. 5. The layout of the heavy ion accelerator facility SIS-ESR is given at the top. The storage and cooler ring, ESR, is depicted for more details in the bottom part (turned by 90°). After injection (1) the ions are cooled by the electron cooler (2). Recombined ions can be detected in a particle counter (3). Opposite to the cooler a gas-jet target can be switched on; down-charged ions may be monitored in a particle detector (5). The insert displays the Schottky noise frequency spectrum of a coasting 295 MeV/u bare Uranium beam before and after cooling.

The electron cooling does not only reduce the emittance of the beam considerably, it fixes also the beam velocity to an absolute constant value, despite small energy losses by collisions with residual gas molecules in the ring. Even if the gas-jet target (4) is switched on the cooling force compensates for the energy loss there. Hence, electron cooling is a prerequisite for precise spectroscopic measurements. Only knowing exactly the accurately

fixed beam velocity vector the Doppler effect can be corrected for.

In the electron cooler ions may also recombine with electrons. These down-charged ions are separated in the next down-stream magnet and can be monitored in a particle detector insertable in a pocket having a thin window (3) [10]. In the same way, ions down-charged in the gas-jet target can be detected (5). The gas jet provides areal densities of 10^{11} to 10^{13} particles per cm^2 of normal gases like nitrogen.

Both, recombination in the cooler or electron capture in the gas target may populate by radiative or to a smaller extend also by non-radiative processes excited projectile levels. For heavy ions these excited states will promptly decay towards the ground-state by characteristic X-ray emission. The Röntgen radiation can be observed by corresponding solid state detectors through thin X-ray windows at the electron cooler at 0° and 180° and at the gas jet at a large variety of angles excluding the smallest forward and backward angles. The X-ray emission is measured in coincidence with the down-charged ions.

X-ray emission and Lamb-shift

The dominant radiative charge-changing processes, radiative recombination (RR) and radiative electron capture (REC), are depicted in Fig. 6. They can be described to some approximation as time-reversed processes of the photo effect [11]. Whereas RR in the cooler corresponds to the inverse threshold photoionization, for REC the kinetic energy of the quasi-free target electrons with respect to the projectile frame has to be added. Moreover, for REC the momentum distribution of the target electrons around their atoms, the "Compton profile" will yield to a broadening of these X-ray transitions. Knowing all the conditions from both RR and REC to the empty K shell, the ground-state binding energy can be inferred [12]. On the other side, RR or REC to excited states populates — either directly or via cascades — the projectile L shell leading to the ground-state transitions shown in Fig. 1. These ground-state x-ray transitions give in the moment a more precise answer to the QED effects enhancing the K level.

As the X-rays are emitted by fast ions the Doppler effect has to be taken into account properly. In particular, large opening angles for detection may yield to unacceptable broadening in the observed line profiles. This is especially true if one does not observe under 0° or 180° where the Doppler shift is largest. In these other cases high-granular detectors have been used, restricting the solid angle per detector segment to tolerable values at simultaneously large total solid angles. In this "Doppler-shift assisted" technique the X-ray spectra from the different segments are individually transformed into the center of mass, *i.e.* into the projectile system, before they are redundantly summed up to one common X-ray spectrum [13].

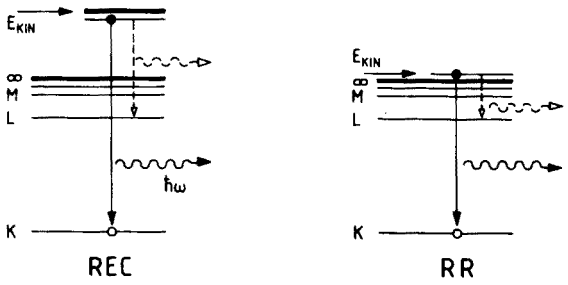

Fig. 6. Radiative charge-changing processes in the cooler and the gas-jet target, radiative recombination "RR" and radiative electron capture "REC", respectively.

In Fig. 7 two X-ray spectra for the neighbouring, initially bare 278 MeV/u Au and 277 MeV/u Pb ions are compared for a spectroscopy at the cooler and the gas-jet target, respectively. As indicated by each experimental arrangement inserted into the figure, the X-ray emission has in both cases taken in coincidence with the down-charged ions; hence, the shown spectra are the characteristic X-ray spectra for the corresponding H-like ions.

In the 0°-lab. spectrum measured at the cooler [14], the Lyman X-ray lines — mainly transitions from the L shell — are observed below the radiative recombination line. At lower X-ray energies the Bremsstrahlung from the cooler dominates. The coincidence spectrum taken at the gas jet displays below the dominant Lyman ground-state transitions the Balmer cascade lines (transitions to the L shell) at around 20 keV [13]. This spectrum has already been transformed into the center of mass system and is detected by seven stripes of a granular detector under 48° in the lab. The dominant Lyman-α lines are at around 80 keV. At the high projectile energy used here, the REC lines are at high X-ray energies far outside the region of the shown spectrum.

From the precise centroid positions of the Lyman-α lines the ground-state Lamb-shift can be deduced. Hence, the X-ray region for the L $\rightarrow$ K ground-state transitions in H-like and He-like Uranium ions is shown in more detail in Fig. 8 at the top and bottom, respectively. These coincident X-ray spectra were taken at the gas-jet target with 295 MeV/u projectiles. Due to electron screening the transition energies in the He-like ions are correspondingly reduced compared to those in the H-like ions. Moreover, in He-like ions one has to deal with a more complicated level diagram and several transitions hide under each line [2]. Therefore, we concentrate in the following to the H-like case, where at least the Lyman-α_1 transition leads to a pure line [15].

From the measured centroid energies of the Lyman-α transitions, the ground-state Lamb-shift was extracted for Uranium in different experi-

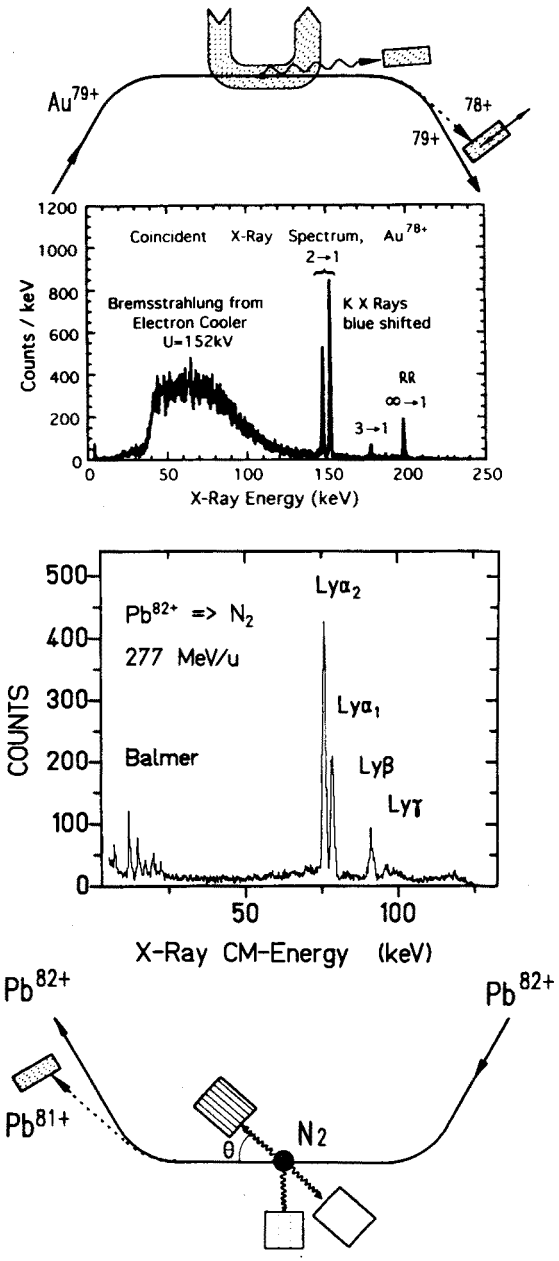

Fig. 7. Coincident X-ray spectra from H-like ions taken for coasting bare (278 MeV/u) Au and (277 MeV/u) Pb projectiles at the electron cooler and the gas-jet target, top and bottom, respectively. The two corresponding experimental arrangements are additionally shown. (For the Au spectrum Lab. energies and for the Pb spectrum CM energies are given.)

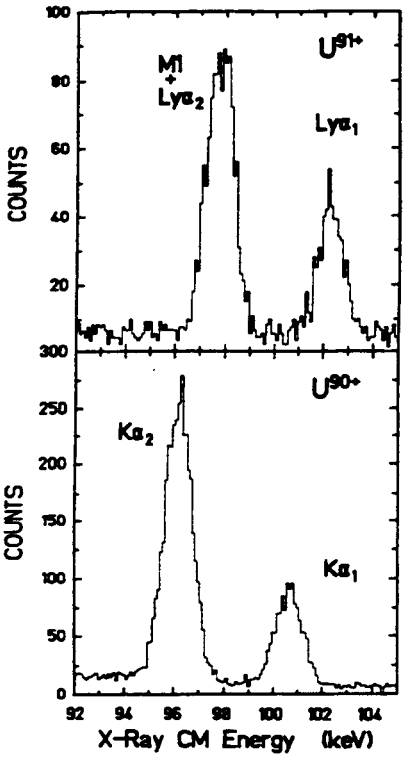

Fig. 8. The ground-state L → K X-ray transitions observed at the gas target for 295 MeV/u Uranium projectiles in coincidence with the down-charged H-like and He-like ions, top and bottom, respectively [2, 15].

ments. In 1990 Briand *et al.* [16] deduced from a measurement at the BEVALAC a value of 520 ± 130 eV. The next test was performed during ESR commissioning at the gas-jet target yielding in 1993 a 1s Lamb-shift of 429 ± 63 eV [15]. With the increased intensities of stored ions in the ESR a more recent measurement at the cooler yielded the most accurate published value of 470 ± 16 eV [17]. This value compares nicely with the theoretical result of Soff [18] (acc. to Ref. [3]) of 463.4 ± 0.6 eV.

It is emphasized that the Lyman-α transition energy in Uranium is about 100 keV, *i.e.* this energy is measured with a precision of 16 eV — or on a 160 ppm level with non-dispersive solid state Ge(i) detectors. That means, presently the ground-state Lamb-shift is determined for H-like Uranium with an accuracy of 3.5 %, confirming the higher $Z\alpha$ contributions of the QED in strong fields. Also for other heavy H-like systems an excellent agreement between experiments and theory was found within the experimental uncertainties. In Fig. 9 the experimental results beyond Argon are compared with the predictions [3] for the Lamb-shift. The $F(Z\alpha)$ function

displayed already in Fig. 3 is compared with the corresponding measurements. The full points beyond $Z = 60$ are all taken at the SIS-ESR facility in Darmstadt, proofing the importance of the higher order terms over the whole range of strong atomic fields.

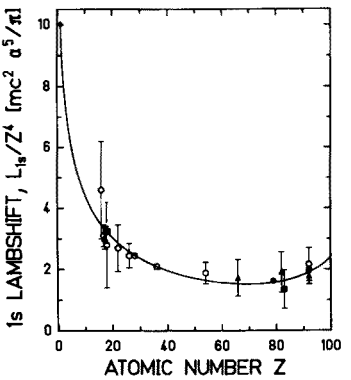

Fig. 9. Comparison of the reduced one-electron ground-state Lamb-shift, $F(Z\alpha)$, with the experimental results. The full data points are results from SIS-ESR; for the other data points *cf.* Ref. [2].

Further developments

The achieved level of accuracy for the ground-state Lamb-shift in H-like ions is indeed remarkable. However, it is still about a factor of 10 above the value claimed for the theoretical uncertainties. Hence, more accurate measurements are needed. One factor crucially limiting the experimental accuracy is the Doppler effect. In order to reduce the influence of this effect one has to reduce the velocity of the stored bare ions actively by applying proper high frequency fields. In a first test experiment bare Uranium ions could be decelerated in the storage ring ESR from 360 MeV/u to 49 MeV/u. At their final energy the ions were cooled by electrons before switching on the gas jet. Then, extremely clean characteristic X-ray spectra with an excellent counting statistics were obtained most recently by Stöhlker *et al.* [19]. These data are currently being analyzed with promising prospects.

For He-like systems it is a lot more difficult to extract QED contributions from the characteristic ground-state transitions, as due to the more complex level diagram the K-α lines are composed lines. Nevertheless, an overall good agreement is reported also here for the Lamb-shift contributions over the whole range of atomic numbers, *cf. e.g.* Ref. [2]. A more promising way seems to be an exploitation of the radiative recombination [20]. There, by comparing simultaneously transitions in H-like and He-like

species of the same atom an equivalent accuracy has been achieved for He-like ions up to Bi. In this ionic stage already the screening of the Lamb-shift has to be considered, *cf.* Ref. [21].

For the experimental accuracy, only a slight improvement by at most a factor of three may be achievable in the limit utilizing solid state detectors and applying the deceleration technique. However, with such an accuracy one starts already to be sensitive on screened Lamb-shift contributions in He-like ions. For H-like ions this may also be the region, where higher order loop contributions in the QED have to be considered. — In this article only one loop diagrams were discussed. — In order to shed more light into this complex field high-resolution spectroscopic methods have to be applied. X-ray crystal spectrometers provide the proper resolution, but including solid angles their detection efficiencies are very small. Hence, their applicability will be limited by the luminosity of the X-ray emission. With the intensities of stored ions available now at the ESR those high-resolution experiments may be feasible in the future. Utilizing also other techniques as Doppler-tuned spectroscopy [22] or cryo-detectors [23] may improve the present experimental accuracy, however, these devices will not reach the ultimate accuracy of crystal spectrometers.

Summarizing, with the measurements performed at the ESR the ground-state Lamb-shift was measured for H-like heavy ions confirming the quantum electro dynamics in strong fields over a wide Z range. In He-like heavy systems the two-electron contributions to the ground-state binding energy were investigated at the super-EBIT [20] also up to very heavy ions. In Both cases, the accuracy of the experiment is not yet good enough to tackle higher order effects like two-loop QED contributions or the two-electron Lamb-shift. However, the higher order $Z\alpha$ QED contributions to the (one-electron) Lamb-shift were nicely confirmed by the studies reported here. There is the hope for even better experimental accuracies in the future giving also answers to the other higher order effects. The new technique of decelerating the ions in the storage ring ESR — which has already been utilized in a very recent experiment — is a first step into this direction.

REFERENCES

[1] W.E. Lamb, R.C. Retherford, *Phys. Rev.* **72**, 241 (1947).
[2] P.H. Mokler, Th. Stöhlker, C. Kozhuharov, P. Rymuza, F. Bosch, T. Kandler, *Phys. Scr. (T)* **51**, 28 (1994).
[3] W.R. Johnson, G. Soff, *At. Data Nucl. Data Tables* **33**, 405 (1985).
[4] P. Indelicato, in *X-Ray and Inner-Shell Processes*, AIP Conf.Proc. 215(1990), p.591.
[5] F. Schmidt-Kaler, D. Leibfried, S. Seel, C. Zimmerman, W. König, M. Weitz, T.W. Hänsch, *Phys. Rev.* **A51**, 2789 (1995).

[6] M.A. Levine, R.E. Marrs, J.N. Bardsley, P. Beiersdorfer, C.L. Bennett, M.H. Chen, T. Cowan, D. Dietrich, J.R. Henderson, D.A. Knapp, A. Osterheld, B.M. Penetrante, D. Schneider, J.H. Scofield, *Nucl. Instrum. Methods Phys. Res.* **B43**, 431 (1989).

[7] R.E. Marrs, S.R. Elliott, D.A. Knapp, *Phys. Rev. Lett.* **72**, 4082 (1994).

[8] H. Poth, *Phys. Rep.* **196**, 135 (1990).

[9] P.H. Mokler, Th. Stöhlker, *Adv. At. Mol. Opt. Phys.* (1995),to be published.

[10] O. Klepper, F. Bosch, H.W. Daues, H. Eickhoff, B. Franzke, H. Geissel, O. Gustafsson, M. Jung, W. Koenig, C. Kozhuharov, A. Magel, G. Münzenberg, H. Stelzer, J. Szerypo, M. Wagner, *Nucl. Instrum. Methods Phys. Res.* **B70**, 427 (1992).

[11] M. Stobbe, *Ann. Phys.* **7**, 661 (1930).

[12] P.H. Mokler, Th. Stöhlker, C. Kozhuharov, Z. Stachura, A. Warczak, *Z. Phys.* **D21**, 197 (1991).

[13] P.H. Mokler, Th. Stöhlker, C. Kozhuharov, R. Moshammer, P. Rymuza, Z. Stachura, A. Warczak, *J. Phys.* **B28**, 617 (1995).

[14] H.F. Beyer, D. Liesen, F. Bosch, K.D. Finlayson, M. Jung, O. Klepper, R. Moshammer, K. Beckert, H. Eickhoff, B. Franzke, F. Nolden, P. Spädtke, M. Steck, *Phys. Lett.* **A184**, 435 (1994).

[15] Th. Stöhlker, P.H. Mokler, K. Beckert, F. Bosch, H. Eickhoff, B. Franzke, M. Jung, T. Kandler, O. Klepper, C. Kozhuharov, R. Moshammer, F. Noldden, H. Reich, P. Rymuza, P. Spädtke, M. Steck, *Phys. Rev. Lett.* **71**, 2184 (1993).

[16] J.P. Briand, P. Chevallier, P. Indelicato, K.P. Ziock, D.D. Dieetrich, *Phys.-Rev.Lett.* **65**, 2761 (1990).

[17] H.F. Beyer, G. Menzel, D. Liesen, A. Gallus, F. Bosch, R. Deslattes, P. Indelicato, Th. Stöhlker, O. Klepper, R. Moshammer, F. Nolden, H. Eickhoff, B. Franzke, M. Steck, *Z. Phys.* **D35**, (1995) in press.

[18] G. Soff, private communication acc. to Ref. [3] (1994).

[19] P.H. Mokler, Th. Stöhlker, R.W. Dunford, A. Gallus, T. Kandler, G. Menzel, H.-T. Prinz, P. Rymuza, Z. Stachura, P. Swiat, A. Warczak, *Z. Phys.* **D35**, (1995) in press.

[20] R.E. Marrs, S.R. Elliott, Th. Stöhlker, *Phys. Rev.* **A52**, 3577 (1995).

[21] I. Lindgren, H. Persson, S. Salomonson, P. Sunnergren, *Phys. Scr.* in print.

[22] J.H. Lupton, D.D. Dietrich, C.J. Hailey, R.E. Stewart, K.P. Ziock, *Phys.Rev.-***A50**, 2150(1994).

[23] D. McCammon, W. Cui, M. Juda, J. Morgenthaler, J. Zhang, R.L. Kelley, S.S. Holst, G.M. Madejski, S.H. Moseley, A.E. Szymkowiak, *Nucl. Instrum.Methods Phys. Res.* **A326**, 157 (1993).